

A Method of Automatic Black Skin Lesion's Macroscopic Image Analysis

Géraud AZEHOUN-PAZOU

LETIA
EPAC 01 BP 2009
Cotonou Rep BENIN

Marc Kokou ASSOGBA

LETIA
EPAC 01 BP 2009
Cotonou Rep BENIN

Antoine VIANOU

LCMAE
EPAC 01 BP 2009
Cotonou Rep BENIN

ABSTRACT

Skin lesions have consistently had one of the most rapidly increasing incidences of all cancers. Early diagnosis is particularly important. However, even with the help of dermoscopy, differentiating malign and benign lesions is a challenging task. More than that, there are many practical situations where only macroscopic imaging is available.

This work focuses on macroscopic images segmentation of black skin lesions. We propose a method combining mathematical morphology and edge detection. After the artifacts extraction stage, we refine the skin lesions by using an opening followed by a dilation algorithm. We then proceed to edge detection. We finally make a comparison of our combination method with existing classical methods.

Keywords

Black Skin Lesions, Mathematical Morphology, Edge Detection, Macroscopic Images.

1. INTRODUCTION

Skin cancer has consistently had one of the most rapidly increasing incidences of all cancers, with 82,770 new cases and 12,650 deaths estimated in the United States in 2013 [1]. Early diagnosis is particularly important since the cancer can be cured if detected in its early stage. Early detection in clinics depends on the so-called ABCD rule to determine the benign or malignant nature of skin lesions. That is, Asymmetry of the lesion's boundaries, Boundary irregularity, Color distributions and lesion Diameters [2]. This fact shows the high dependency of the correct diagnosis on the observer's experience and on his or her visual acuity. Moreover, the human vision lacks accuracy, reproducibility and quantification in gathering information from an image while the use of digital image features may help in an objective follow up study of skin lesion progression and test the efficacy of therapeutic procedures [3][4].

There are two types of skin lesion images: macroscopic images and dermoscopic images. Macroscopic skin lesion image is a conventional clinical image captured with an ordinary CCD camera.

To help diagnosing pigmented skin lesion, physicians often use dermoscopy which is a non-invasive skin imaging technique that uses optical magnification and either liquid immersion and low angle-of-incidence lighting or cross-polarized lighting to make the contact area translucent, making subsurface structures more easily visible when compared to conventional macroscopic images [5].

According to Celebi et al [6], one of the most important features for the diagnosis of melanoma in dermoscopy images

is the blue-white veil (irregular structureless areas of confluent pigmentation with an overlying white "ground-glass" film). So, authors present a machine learning approach to the detection of blue-white veil and related structures in dermoscopy images. The method involves contextual pixel classification using a decision tree classifier.

The boundary irregularity of skin lesions is of clinical significance for the early detection of malignant melanomas and to distinguish them from other lesions such as benign moles. Ma and Staunton [7] proposed an approach of solution to this problem, which consist in characterizing structural components of contour. To extract this structure from the contour, wavelet decomposition has been used as these components tend to locate in lower frequency sub-bands [7]. Lesion contours were then modeled as signatures with scale normalization to give position and frequency resolution invariance. After that, energy distributions among different wavelet sub-bands were analyzed to extract those with significant levels and differences to enable maximum discrimination [7].

Based on the coefficients in the significant sub-bands, structural components from the original contours were modeled, and a set of statistical and geometric irregularity descriptors were applied at each of the significant sub-bands. Effectiveness of the descriptors was measured using the Hausdorff distance between sets of data from melanoma and mole contours.

Other innovative tools for skin analysis are the vibration spectroscopic techniques. They are based on the non-destructive light-matter interaction and allow extraction of a "molecular fingerprint" characteristic of the analyzed sample pathological state. Ly et al. [8] performed an evaluation of these techniques.

In a general approach to help in processing of dermoscopic images, a pre-processing scheme was proposed by Madooei et al. [9]. The contributions are two-fold. First, a procedure is proposed to facilitate the detection and removal of artifacts such as hairs. Second, a novel simple grayscale conversion approach is presented. It is based on physics and biology of human skin and provides high separability between a pigmented lesion and normal skin surrounding it.

According to Mayer [10], the use of dermoscopy can increase the sensitivity in 10-27% with respect to the clinical diagnosis. Also, several automatic segmentation and classification methods have been proposed to help obtain a diagnosis with a dermoscopy image [11-16].

However, even with the help of dermoscopy, differentiating malign and benign lesions is a challenging task. In fact, specialists affirm that in the early evolution stages of malignant lesions, dermoscopy may not be helpful since it

often does not improve the diagnosis accuracy at this stage [17]. Still considering early cases, there are practical situations where a non-specialist wishes to have a qualified opinion about a suspected skin lesion, but only standard camera imaging is available on site. Many other situations exist where specialists themselves don't have adequate equipments like dermoscopy, particularly in very poor countries.

In our knowledge, there is not enough work done specifically on black skin macroscopic images in terms of automatic analysis. Antoine Mahé published in 1998 some images in his book "Skin diseases in Bamako (Mali)" [18]. Puigdemont et al., [19] presented a book on "Dermatology in patients with black skin". Before them, others like Basset [20] or Wallach [21] had addressed some aspects of the topic. Let's notice that above works deal with analog images.

Usually, the typical computer-aided diagnosis pipeline adopted for automated skin lesion diagnosis is image acquisition, artifact detection, lesion segmentation, feature extraction and classification [22]. In this paper, we present a method of automatic analysis of macroscopic images of black skin lesion, based on image segmentation. The method is a combination of mathematical morphology and classical edge detection algorithms. In the artifact detection stage we use median filtering. In the segmentation stage, classical opening and dilatation algorithms are used followed by edge detection.

The remainder of this paper is organized as follows. Section 2 describes the material and the method. Section 3 presents the results. In section 4 we present a discussion and finally, we conclude in section 5.

2. MATERIEL AND METHOD

2.1. Materiel

The images used are from [18-19] and [23]. On figure 1, some of them are presented: images 1-a and 1-b are erythema, image 1-c is eczema at the elbow, on image 1-d we have profused hypochromiantes eczematides in an infant.

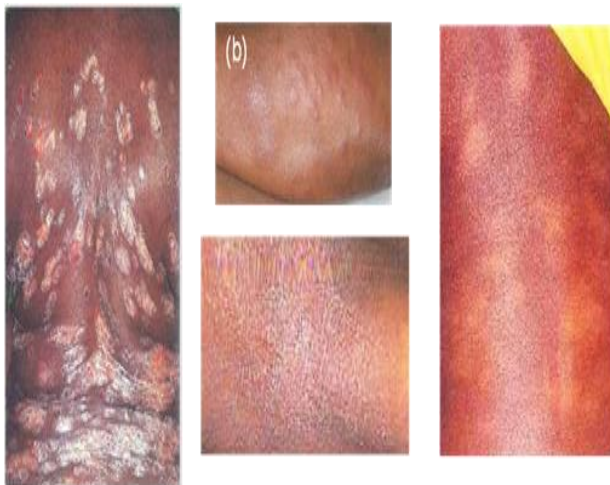


Fig 1: Black skin lesions images

The algorithms are implemented using MATLAB 7.10.

2.2. Methods

We show the procedure in figure 2 and its details in the following sub-sections.

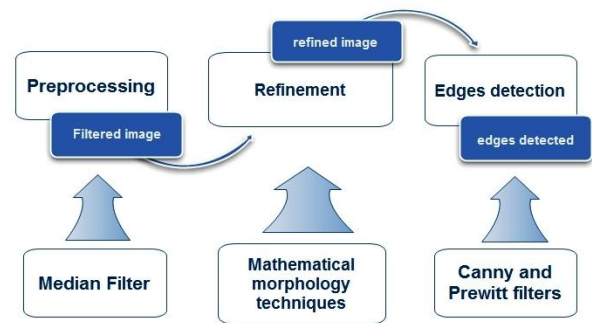


Fig 2: Proposed segmentation procedure

2.2.1. Preprocessing

Image analysis process usually begins with artifacts extraction. At this stage, we use median filter with filters windows size of 3X3 and 5X5. The choice of this type of filter is justified by the nature of noise present and especially the small difference of pixel values in the images.

Indeed, the median filter belongs to the class of non-linear filters, which unlike linear filters prevent spreading transitions between regions in filtered image. Its functioning consists in replacing a pixel value by the median value of its neighborhood pixels. It proceeds to do a sort of gray level values in the neighborhood followed by selection of the middle of sorting elements.

Let $f(x_o, y_o)$ be the value of a pixel X in the image and $f(x_i, y_i)$ the value of any pixel X_i around X with $i=1, 2, \dots, N$. In a window of size 3x3, $N=9$ and in a window of size 5x5, $N=25$. We sort the N values such that the smallest value is f_1 and the highest is f_N as shown in figure 3.

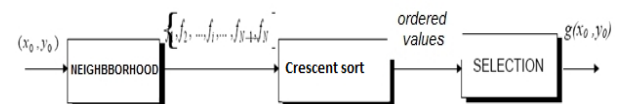


Fig 3: Median filter process

We have $f_1 < f_2 < \dots < f_{(N+1)/2} < \dots < f_{N-1} < f_N$, and the median value is $f_{(N+1)/2}$.

2.2.2. Refinement

Differences of pixels in the images are very small. To better illustrate objects, we refine their shapes. To do this, we use mathematical morphology algorithms, whose techniques proceed to description of objects shapes by comparing them with objects whose shapes are well known, the structuring elements. We realize openings of each image used. Indeed, opening acts as filter on binary images. It helps soften edges, cut the narrow isthmus, eliminates small islands and narrow caps.

The opening of an X picture by a structuring element B is realized by performing an erosion of X by B, followed by a dilation of X by the transposed Bt of B:

$$O^B(X) = D^{B^t}(E^B(X)) \quad (2.1)$$

The structuring elements we used are convex objects such as segment and disk.

Regarding the eroded Y of a set X by a structuring element B, it is defined as the set of points x of X such as B is entirely contained in X when it is centered on x:

$$Y = E^B(X) = \{x \in X / B_x \subset X\} \quad (2.2)$$

Thus the structuring element B identified by its center, is successively moved to occupy all positions of the space E. For each position, if B is completely included in X, then the pixel selected is part of the eroded set.

As far as the expanded Z of X by B is concerned, it is the set of points x of X such as at least one point of B is in contact with X, when it is centered on x:

$$Z = D^B(X) = \{x \in X / X \cap B_x \neq \emptyset\} \quad (2.3)$$

Thus, the structuring element B is moved to occupy all positions of the space E, successively. For each position, we ask the question: "does B intersect X?" The positive answers form the expanded set. The structuring element used to make mathematical morphological processing of the image is a disk.

2.2.3. Edges detection

The aim of our study is to segment black skin lesions images. We use edge detection approach because in dermatological approach, factors such as size, shape, distribution, are of some interest. To do this, Canny and Prewitt methods have been applied to each image.

2.2.3.1. Prewitt method

This method calculates light intensity gradient on the image at each point, giving direction and rate of the largest decline. The result indicates abrupt changes in brightness on the image and thus exhibits its likely contours. In practice this technique is more reliable and easier to implement than a more direct algorithm. Mathematically, the filter of this method is composed of two 3x3 matrices which are convolved with the original image to calculate an approximation of its derivative at any point. The first matrix calculates the horizontal derivative and the second gives the vertical derivative. If we define A as the source image, G_x and G_y as horizontal and vertical derivative images of the luminous intensity of the image, we can thus calculate them with the following 2d convolution operations:

$$G_x = \begin{bmatrix} -1 & 0 & +1 \\ -1 & 0 & +1 \\ -1 & 0 & +1 \end{bmatrix} * A \quad \text{and} \quad G_y = \begin{bmatrix} +1 & +1 & +1 \\ 0 & 0 & 0 \\ -1 & -1 & -1 \end{bmatrix} * A \quad (2.4)$$

Prewitt method is preferred to Sobel one, which uses same technique, but it implements a more rectangular smoothing that introduces phase changes during processing. Thereby possible noise is attenuated.

2.2.3.2. Canny method

The operator used here calculates the gradient in X and Y directions. It is composed of two convolution masks, one of dimension 3x1 and the other 1x1:

$$G_x = \begin{bmatrix} 1 & 0 & 1 \end{bmatrix} \quad G_y = \begin{bmatrix} 1 \\ 0 \\ -1 \end{bmatrix} \quad (2.5)$$

$$\theta = \tan^{-1} \left(\frac{G_y}{G_x} \right) \quad (2.6)$$

Gradient value at a point is approximated by formula: |G| = |G_x| + |G_y| (2.7). The guidance outlines are determined by formula (2.6). We finally get a map of the intensity gradients at each point along the directions of picture contours. This board provides intensity at each point of the image. A high intensity indicates a high probability of

presence of a contour. However, this intensity is not sufficient to decide whether a point is an outline or not. Only those corresponding to local maxima are considered as corresponding to contours, and are kept.

To perform this differentiation, contours on the map, a hysteresis thresholding is used. This requires two levels (high and low) that will be compared to the gradient intensity of each point. The decision criterion is the following: for each point, if the gradient intensity:

- is less than the low threshold, the point is rejected
- exceeds the upper threshold, the point is accepted, then forming a contour;

Once this step is completed, the obtained image is binary with one side of the pixels belonging to the contours. This method is of interest to us because it gives the best results in the three following criteria:

- good detection: low error rate in contours signaling,
- good localization: minimization of distance between detected edges and actual contours
- clarity of the answer: one response outline and no false positives.

3. RESULTS

Figure 4-a represents grayscale image of an erythema revealed during psoriasis (figure 1-a lesion). Figures 4-b and 4-c are results obtained after edge detection respectively with Prewitt and Canny methods. For both methods, the result is not optimal because there is a part of non-existent boundaries that have been created (Canny) and non-detected contours (Prewitt). While, we have better results with both CMP (figure 4-d) and CMC (figure 4-e) methods.

In order to assess the efficiency of different methods, we counted the number of edges points detected with each method. Different values are exposed in table 1.

Table 1. Comparison between conventional methods and combined methods for edges detection on lesion 1-a

METHODS	PREWITT	CANNY	PROPOSED METHOD	
			CMP	CMC
NUMBER OF EDGE POINTS	9208	26945	11530	12551

LEGEND:

CMP: Combination of mathematical morphology and Prewitt filter
 CMC: Combination of mathematical morphology and Canny filter

Figure 5-a is the image of an erythema of intermediate shade barely visible to naked eye, which could be misjudged by practitioners. Despite small difference of pixel values between healthy parts and those affected, good result is obtained with combined methods. On the contrary, when edges points are detected without mathematical morphological processing, we have not accurate results (figures 5-c and 5-d). Table 2 shows number of edge points detected with various methods.

Table 2. Comparison between conventional methods and combined methods for edges detection on lesion 1-b

METHODS	PREWITT	CANNY	PROPOSED METHOD	
			CMP	CMC
NUMBER OF EDGE POINTS	2151	21584	5562	4368

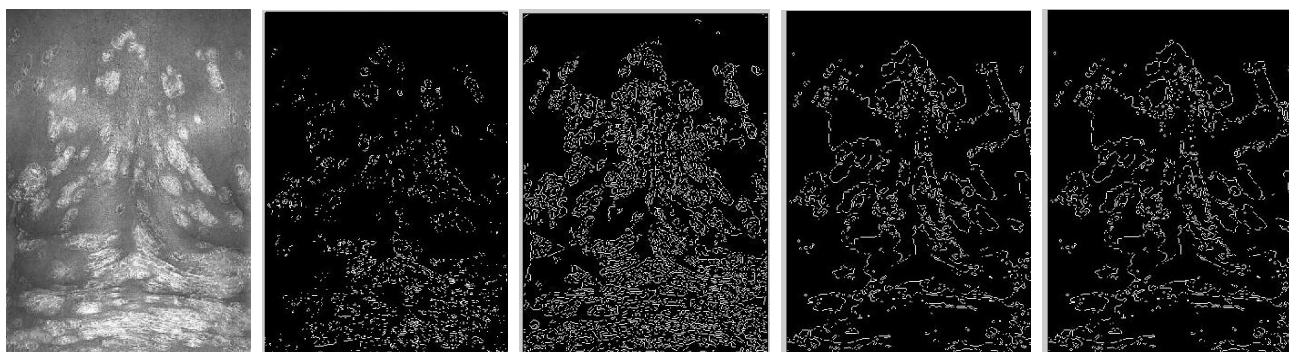


Fig 4: Results obtained on a black skin erythema image

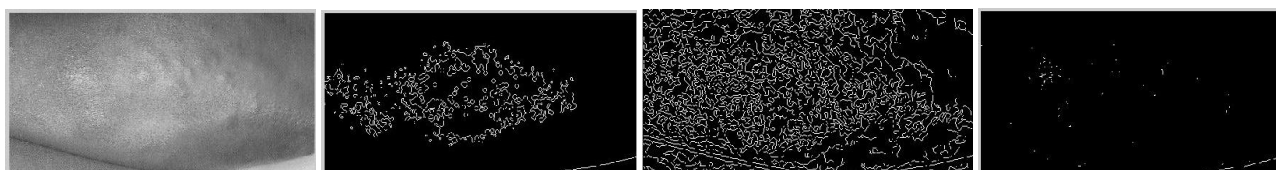


Fig 5: Results obtained on an erythema of intermediate shade on black skin image

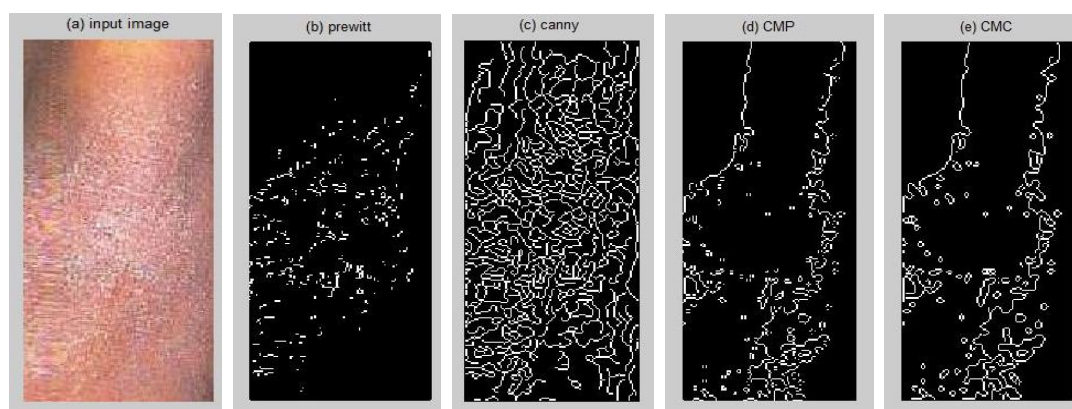


Fig 6: Results obtained on an image of eczema at elbow

Figure 6 also shows difference between a statement made directly segmentation and segmentation made after morphological processing. The lesion here is eczema present at the elbow of a subject. Table 3 shows number of edges points found on the lesion 1-c using different methods.

Table 3. Comparison between conventional methods and combined methods for edges detection on lesion 1-c

METHODS	PREWITT	CANNY	PROPOSED METHOD	
			CMP	CMC
NUMBER OF EDGE POINTS	743	4495	1351	1576

Figure 7 illustrates relative differences of edge points numbers detected with each methods. We can see through this graph that obtained results with standard methods (Prewitt and Canny) are not accurate for contours detection on black skin lesions images. On the other size, the proposed method, which combines mathematical morphology tools with both Prewitt (CMP) and Canny (CMC) methods, the results are much more accurate.

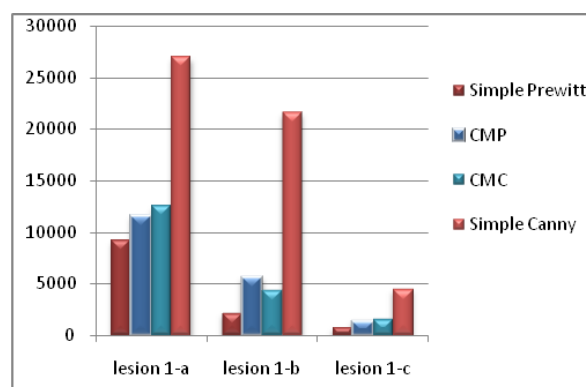


Fig 7: Edges detection with classic methods and combined methods using mathematical morphology

4. DISCUSSION

It emerged from the results obtained that introduction of mathematical morphology tools in segmentation process, yielded relevant results on black skin lesions images. Let's note that the proposed procedure is also efficient on white skin lesions images.

Nevertheless, it should be noted that the procedure is not perfect. An illustration is the result obtained with the lesion of figure 8, where some parts of the lesion (circled in yellow) have not been detected.



Fig 8: Result obtained with proposed method on lesion 1-d

5. CONCLUSION

This study identified the significant differences that exist between black skin and white skin. These differences can firstly be observed in terms of color secondly in anatomical and structural terms, etc. They induce some difficulties to dermatology practitioners, as seen in various publications that have been made on the subject especially during the last decade.

This little interest for black skin lesions from scientists, motivate our research whose goal is to establish an adapted procedure for black skin lesions image segmentation. To do this, we first do some research on existing conventional methods of segmentation, and then discuss mathematical morphology concepts. We finally designed and tested a procedure combining mathematical morphology techniques and edges detection approach.

6. ACKNOWLEDGMENTS

Authors would like to thank Doctor Hugues ADEGBIDI of National University Hospital (CNHU HKM) of Cotonou Benin for his help in the work.

7. REFERENCES

- [1] Siegel R., Naishadham D., Jemal A. 2013. "Cancer Statistics, 2013". CA: A Cancer Journal for Clinicians, 63(1): 11-30.
- [2] Grana C., Pellacani G., Cucchiara R., Seidnari S. 2003. "A new algorithm for border description of polarized light surface microscopic images of pigmented skin lesions." IEEE Transactions on Medical Imaging 22(8) 959-964.
- [3] Hansen G., Sparrow E., Kokate J. 1993. "Wound status evaluation using color image processing." IEEE Transactions on Medical Imaging, 12, 1, 39-43.
- [4] Nishik M., Foster C. 1997. "Analysis of Skin Erythema Using True Color Images." IEEE Transactions on Medical Imaging, 16, 6, 711-716.
- [5] Menzies S.W., Crotty K. A., Ingwar C., McCarthy W.H. 2003. "An Atlas of Surface Microscopy of Pigmented Skin Lesions: Dermoscopy." Sydney, Australia: Mc Graw-Hill.
- [6] Celebi M. E., Iyatomi H. Stoecker W. V., Moss, R. V., Rabinovitz H. S., Argenziano G. Soyer P.H. 2008. "Automatic detection of blue-white veil and related structures in dermoscopy images." Computerized Medical Imaging and Graphics. 32 pp 670-677.
- [7] Ma, L., Staunton, R. C. 2013. "Analysis of the contour structural irregularity of skin lesions using wavelet decomposition." Pattern Recognition, 46, pp.98-106.
- [8] Ly, E., Piot, O., Wolthuis, R., Durlach, A., Bernard, P., & Manfait, M. 2008. "Combination of FTIR spectral imaging and chemometrics for tumour detection from paraffin-embedded biopsies" Analyst, 133(2), pp. 197-205.
- [9] Madooei A., Drew MS., Sadeghi M., & Atkins, M. S., 2012 "Automated Pre-processing Method for Dermoscopic Images and its Application to Pigmented Skin Lesion Segmentation" Color and Imaging Conference, CIC, Los Angeles.
- [10] Mayer J. 1997. "Systematic review of the diagnostic accuracy of dermatoscopy in detecting malignant melanoma." Med J Aust 167:206-210
- [11] Celebi M.E., Kingravi HA., Uddin B., Iyatomi H., Aslandogan, Y.A., Stoecker, W.V., Moss, RH. 2007. "A methodological approach to the classification of dermoscopy images." Comput Med Imaging Graph 31(6):362-373
- [12] Celebi ME, Kingravi HA, Iyatomi H, Aslandogan YA, Stoecker WV, Moss RH, Malters JM, Grichnik JM, Marghoob AA, Rabinovitz HS, Menzies SW 2008. "Border detection in dermoscopy images using statistical region merging." Skin Res Technol 14:347-353.
- [13] Gomez DD, Butakoff C, Ersboll BK, Stoecker W 2008. "Independent histogram pursuit for segmentation of skin lesions". IEEE Trans Biomed Eng 55:157-161.
- [14] Iyatomi H, Oka H, Celebi M, Hashimoto M, Hagiwara M, Tanaka M, Ogawa K 2008. "An improved internet-based melanoma screening system with dermatologist-like tumor area extraction algorithm." Comput Med Imaging Graph 32(7):566-579.
- [15] Zhou H, Schaefer G, Sadka A, Celebi M. 2009. "Anisotropic mean shift based fuzzy c-means segmentation of dermoscopy images." IEEE J Sel Top Signal Process 3:26-34.
- [16] Zhou H, Schaefer G, Celebi ME, Lin F, Liu T. 2011. "Gradient vector flow with mean shift for skin lesion segmentation." Comput Med Imaging Graph 35(2):121-127.
- [17] Skvara H, Teban L, Fiebigler M, Binder M, Kittler H., 2005. "Limitations of dermoscopy in the recognition of melanoma." Arch Dermatol 141:155-160.
- [18] Mahé A., Cissé IA., Faye O., N'diaye HT., Niamba P., 1998. "Skin diseases in Bamako (Mali)." Intv J Dermatol 1998 (37), pp. 637 - 646.
- [19] Puigdemont, G. S., Sintes, R. N., Dieng, T. 2008. "Dermatology with black skin patients." Euromedice 308p.
- [20] Basset, A., 1966. "Dermatological problems of black skin." Rev Pratt 1966 (16), pp. 2087-2097.

- [21] Wallach D., 1981. "Specific aspects of dermatological diagnosis on black skin." *Rev. Pratt* 1981, pp. 3675-3688.
- [22] Wighton P., Lee T. K., Lui H., Mclean D.I., Atkins S. M. 2011. "Generalizing Common Tasks in Automated Skin Lesion Diagnosis." *IEEE Transactions on Information Technology in Biomedicine*, Vol. 15, No. 4, 2011.
- [23] Djogbénou, I. G. F., 2012. *Dermatoses in preschool children: epidemiological and clinical aspects in the department of dermatology, venereology of CNHU-HKM, Cotonou*. PhD thesis, Faculty of health sciences, University of Abomey-Calavi (Benin), 115p.